ASTROBIOLOGY
Volume 12, Number 4, 2012

DOI: 10.1089/ast.2011.0754

Nitrogen Incorporation in CH_4-N_2 Photochemical Aerosol Produced by Far Ultraviolet Irradiation

Melissa G. Trainer,[1] Jose L. Jimenez,[2] Yuk L. Yung,[3] Owen B. Toon,[4] and Margaret A. Tolbert[2]

Abstract

Nitrile incorporation into Titan aerosol accompanying hydrocarbon chemistry is thought to be driven by extreme UV wavelengths ($\lambda < 120$ nm) or magnetospheric electrons in the outer reaches of the atmosphere. Far UV radiation (120–200 nm), which is transmitted down to the stratosphere of Titan, is expected to affect hydrocarbon chemistry only and not initiate the formation of nitrogenated species. We examined the chemical properties of photochemical aerosol produced at far UV wavelengths, using a high-resolution time-of-flight aerosol mass spectrometer (HR-ToF-AMS), which allows for elemental analysis of particle-phase products. Our results show that aerosol formed from CH_4/N_2 photochemistry contains a surprising amount of nitrogen, up to 16% by mass, a result of photolysis in the far UV. The proportion of nitrogenated organics to hydrocarbon species is shown to be correlated with that of N_2 in the irradiated gas. The aerosol mass greatly decreases when N_2 is removed, which indicates that N_2 plays a major role in aerosol production. Because direct dissociation of N_2 is highly improbable given the immeasurably low cross section at the wavelengths studied, the chemical activation of N_2 must occur via another pathway. Any chemical activation of N_2 at wavelengths >120 nm is presently unaccounted for in atmospheric photochemical models. We suggest that reaction with CH radicals produced from CH_4 photolysis may provide a mechanism for incorporating N into the molecular structure of the aerosol. Further work is needed to understand the chemistry involved, as these processes may have significant implications for how we view prebiotic chemistry on early Earth and similar planets. Key Words: Titan—Photochemical aerosol—CH_4-N_2 photolysis—Far UV—Nitrogen activation. Astrobiology 12, 315–326.

1. Introduction

It has been assumed that the photolysis of CH_4/N_2 in the far ultraviolet (FUV), 120–200 nm, would not lead to any nitrogen chemistry due to the difficulty in breaking the N_2 triple bond. Nitriles have been observed on Titan in the thermosphere (Vuitton *et al.,* 2007) and throughout the stratosphere (Coustenis *et al.,* 2007), but the initial formation of the –CN bond is assumed to take place only in the ionosphere, largely from extreme ultraviolet (EUV) photons or the impact of high-energy electrons present in Saturn's magnetosphere (Yung *et al.,* 1984). Recent work by Imanaka and Smith (2010) has shown that photoionization initiated by EUV photons ($\lambda < 120$ nm) can lead to nitrogen fixation via the production of the HCCN radical, with a substantial portion of the nitrogenated products partitioning into the solid aerosol phase. These processes would occur mainly above 1000 km in Titan's atmosphere (Sagan *et al.,* 1992).

The photon flux at Ly-α (121.6 nm) and other wavelengths longward of 120 nm is orders of magnitude greater than at the EUV, and the longer wavelength light has a greater penetration depth into the atmosphere (Wilson and Atreya, 2004). However, because the nitrogen chemistry for Titan is thought to be fully accounted for by N_2 dissociation processes in the upper atmosphere (Vuitton *et al.,* 2007; Lavvas *et al.,* 2011), the possibility of chemical activation of N_2 in the FUV has not been carefully examined. Nitrogen activation in the FUV could have exciting implications for prebiotic chemistry on early Earth and other planetary bodies. Dodonova (1966) found that HCN could be formed via

[1]NASA Goddard Space Flight Center, Greenbelt, Maryland.
[2]Department of Chemistry and Biochemistry and Cooperative Institute for Research in Environmental Sciences, University of Colorado at Boulder, Boulder, Colorado.
[3]Division of Geological and Planetary Sciences, California Institute of Technology, Pasadena, California.
[4]Laboratory for Atmospheric and Space Physics and Department of Atmospheric and Oceanic Sciences, University of Colorado at Boulder, Boulder, Colorado.

irradiation of CH_4/N_2 mixtures at wavelengths >125 nm, but successive attempts to replicate these results by using UV line sources were unsuccessful (see Table 1, Raulin *et al.*, 1982). Given the null results, Raulin *et al.* (1982) summarized that the only contribution of FUV radiation on a CH_4/N_2 atmosphere was the production of hydrocarbons. To simulate the incorporation of nitrogen into solid haze material photochemically, other workers have used HCN and HC_3N in initial gas mixtures (Clarke and Ferris, 1997; Tran *et al.*, 2008).

In previous work by our group, the aerosol product of CH_4/N_2 photochemistry at $\lambda > 115$ nm was examined for chemical composition, physical properties, and mass production rates with a variety of analytical techniques, including a unit mass resolution aerosol mass spectrometer (Trainer *et al.*, 2006). The aerosol mass production rate within the photochemical cell was characterized by varying the concentration of CH_4 in N_2, and the resulting rate of aerosol production was shown to represent a significant source for the delivery of organic material to the early Earth environment given predicted CH_4 abundances and photon fluxes for the young planet (Trainer *et al.*, 2006). For the chemical analysis, the assumption was made that nitrogen chemistry could be ignored and the aerosol product consisted solely of hydrocarbon material. Here, we revisit the CH_4/N_2 experiment, using a high-resolution time-of-flight aerosol mass spectrometer (HR-ToF-AMS) to more closely examine the chemical composition of the aerosol products. The use of the HR-ToF-AMS allows us to provide new insights into the chemical composition of the photochemical aerosol and the role of atmospheric N_2 in aerosol formation.

2. Materials and Methods

The photochemical flow reactor used to generate the aerosol has been described extensively in previous work (Trainer *et al.*, 2006; DeWitt *et al.*, 2009; Hasenkopf *et al.*, 2010). In the present work, the gas mixture preparation and aerosol generation procedures were followed precisely as described previously for interfacing with the aerosol mass spectrometer (AMS) (Trainer *et al.*, 2004a, 2004b, 2006). Briefly, a mass flow controller (Mykrolis, FC2900) was used to flow prepared gas mixtures at a rate of 100 standard cm^3 min^{-1} through a 300 cm^3 glass reaction cell and into the inlet of the AMS. A water-cooled deuterium lamp (Hamamatsu, L1835) with MgF_2 windows, emitting from 115 to 400 nm, was inserted directly into the reaction cell. The deuterium lamp is a continuum source but has a peak near 121 nm, analogous to the solar Ly-α line at 121.6 nm, which is a primary driver of CH_4 photolysis in planetary atmospheres. The reaction cell was held at close to room pressure (~600 torr) and room temperature, as measured by an in-line 1000 torr Baratron (MKS, 626A) and thermocouples attached to the exterior of the reaction cell.

The work described here builds upon previous studies in which the chemical and physical properties of photochemical haze aerosol produced from CH_4/N_2 mixtures were extensively characterized (Trainer *et al.*, 2006). Inherent in the previous work was an assumption that the N_2 molecules were not photolyzed at the experimental wavelengths and, therefore, served only as third bodies for reactions and did not become chemically incorporated in the aerosol molecular structure. To examine the validity of this assumption, the photochemical study was expanded to include high-resolution chemical analysis to explore the effect of the composition of the background gas. Gas mixtures were prepared in which the CH_4 mixing ratio was held constant at 0.1%, and the N_2 concentration was varied in a background gas of argon (Ar). Gas reagents used were acquired from Airgas, Inc. (Radnor, PA) with minimum purities of 99.99, 99.999, and 99.998% for CH_4, N_2, and Ar, respectively. The CH_4 mixing ratio is lower than that on Titan but is based on past experience with the photochemical cell and optimization of aerosol productivity. Our previous work showed that, as the CH_4/N_2 ratio was varied in the gas mixture, the chemical composition of the aerosol did not change, but higher production rates were observed at 0.1% than at 2% (Trainer *et al.*, 2006). Thus, the lower mixing ratio was used in the present study to ensure the best signal-to-noise ratio in our measurements.

The following experiments were performed, described by the fractional concentration of N_2 (with Ar bringing the total pressure to 600 torr): 0, 0.01, 0.1, 0.6, 1, 5, 31, 66, and 100% N_2. In addition, one experiment was performed with CH_4 with helium (He) as the background gas but no N_2 present. Each gas mixture was cycled through a minimum of three photochemical experiments lasting 1–2 h each. An experiment consisted of first establishing a flow of the gas mixture through the reaction cell and into the mass spectrometer with no irradiation, which provided a procedural background measurement. The light source was then turned on to initiate

Table 1. Comparison of Results for Previous CH_4/N_2 Photolysis in Far UV

Wavelength range (nm)	*Reference*	*Reaction pressure (torr)*	*Products reported (phase)*
125–170	Dodonova, 1966	5–8, 100–200	HCN (gas)
123.6	Chang *et al.*, 1979	*not specified*	Organics, No N-containing (gas)
147	Bossard, 1979 *from* Bossard *et al.*, 1982	10	Organics, No N-containing (gas)
184.9	Ferris and Chen, 1975	670	Organics, No N-containing (gas)
112–135	Scattergood *et al.*, 1989	*not specified*	HCN, hydrocarbons (gas)
50–150	Imanaka and Smith, 2007	0.05	Organics produced at Ly-α (gas) but with reduced efficiency than lower λ, N chemistry uncertain
115–400	This work	600	Nitriles, –CN linkages (solid)

photochemical aerosol production, and aerosol product was observed in the mass spectrometer within 5–10 min. A steady production rate was typically achieved within 20 min. The averaged spectra shown in this manuscript represent this steady state.

The distinguishing element of this study is the use of the HR-ToF-AMS for chemical analysis of the photochemical aerosol (DeCarlo *et al.,* 2006). All previous work by this group on CH_4/N_2 photochemical hazes was conducted with a unit-resolution quadrupole AMS (Q-AMS). While the data produced from the Q-AMS was extremely valuable in the assessment of the chemical trends of the aerosol as a function of trace gas composition (*e.g.,* CH_4, CO_2, H_2), the high mass resolution of the HR-ToF-AMS allowed for the first definitive evaluation of the nitrogen content in the aerosol product. The sample introduction system, particle sizing, and vaporization and ionization systems of the HR-ToF-AMS are the same as those of the Q-AMS used previously (Canagaratna *et al.,* 2007). Following ionization, the generated ions are extracted into a high-resolution, time-of-flight mass spectrometer (H-TOF Platform, from Tofwerk, in Thun, Switzerland). Ions of different mass-to-charge ratio (*m/z*) values achieve different velocities when they are extracted into the flight path and, therefore, are separated by flight time when they impact on the microchannel plate detector. All data presented here were collected with the HR-ToF-AMS ion optics operating in the "W-mode" (named after the shape of the ion path) of the spectrometer, which increases the flight path and improves ion separation and consequently mass resolution, but with reduced sensitivity (DeCarlo *et al.,* 2006). In this mode, the resolving power of the instrument ranges from $m/\Delta m = 3000$ to 4300 over the *m/z* range of interest (10–200), and the mass accuracy has been estimated at approximately ±7 ppm. Here, only averaged compositional data derived from the mass spectrum (MS) mode are presented.

Custom software was used to analyze the HR-ToF-AMS data in Igor Pro 6.1 (Wavemetrics, Lake Oswego, OR). The algorithms applied to the data for performing the *m/z* calibration, Gaussian fit of ion peaks, and extraction of ion intensities for elemental analysis have been described in detail in the literature (DeCarlo *et al.,* 2006; Aiken *et al.,* 2007, 2008) and are included in the analysis software. The total ion current of each ion is determined based on the signal peak area (not peak height) in the spectrum. The custom peak-fitting routine fits each ion peak with a modified Gaussian shape that is a function of the ion time of flight and applies an array of user-defined possible ions (exact *m/z* values) to allow for identification and quantification of the ion signal regardless of the occurrence of overlapping ion peaks at each integer *m/z* (DeCarlo *et al.,* 2006). Two recent studies report good agreement of the elemental analysis results of HR-ToF-AMS data with those from other techniques (Chhabra *et al.,* 2010; Kroll *et al.,* 2011).

3. Results

The average aerosol mass spectrum for the 0.1% CH_4/N_2 photochemical product is displayed with unit resolution in

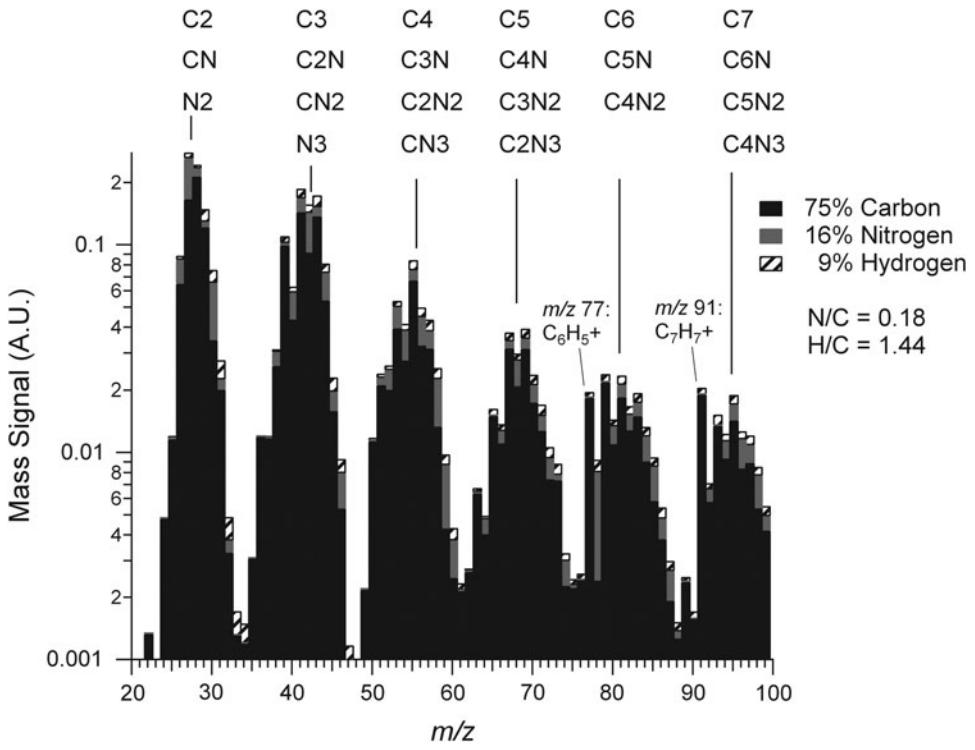

FIG. 1. Elemental analysis from the high-resolution mass spectrum of Titan aerosol analogues produced from photochemistry of 0.1% CH_4 in N_2 background gas. These results show a substantial fraction of nitrogen included in the aerosol material by mass. Atomic ratios are indicated in the legend. The mass spectrum shows fragmentation patterns typical of unsaturated hydrocarbons with amine and/or nitrile groups. The figure includes the lists of skeletal formulas (without H) indicated by the high-resolution mass spectra of the integer *m/z* for each group of peaks on the "picket fence," showing a variety of molecular fragments. A.U., arbitrary units.

Fig. 1. The spectrum is fundamentally similar to that obtained with the Q-AMS and presented in the previous publication (Trainer *et al.,* 2006). A comparison of the two spectra yields an $R^2 = 0.90$, which is consistent with the level of reproducibility of AMS spectra across instruments (Dzepina *et al.,* 2007). As discussed in the previous work, the pattern observed indicates that the aerosol contains unsaturated hydrocarbons with varying chain lengths. Aromatic indicators (fragments at *m/z* 77 and 91 for phenyl and benzyl ions, respectively) are also observed.

A surprising finding revealed in the high-resolution measurement is a substantial nitrogen component in the organic aerosol structure. Figure 2 shows the region of the spectrum around the nominal *m/z* 27, which was previously assumed to arise solely from a hydrocarbon (*i.e.,* $C_2H_3^+$) fragment ion. The high-resolution spectrum retrieved from the high-resolution time of flight and peak-fitted as discussed above (DeCarlo *et al.,* 2006) shows that more than half the signal at this integer *m/z* arises from an ion peak centered around *m/z* 27.011, which is attributed to the HCN^+ ion (exact *m/z* 27.01035). The remainder of the signal is due to the peak from the hydrocarbon fragment $C_2H_3^+$ (exact *m/z* 27.02293). We calculate that a minimum $m/\Delta m$ value of 2148 at full width at half-maximum is needed to adequately separate these peaks, and this criterion is met by the minimum instrument resolving power of 3000.

The spectrum is similarly fitted at each nominal *m/z* in the range from 20 to 100, where most (88%) of the aerosol signal appears, and the elemental composition of each ion is combined with the measured ion currents to determine the bulk elemental composition for the average aerosol spectrum. This compositional analysis allows for a calculation of the relative mass concentrations of the major elemental species carbon (C), nitrogen (N), and hydrogen (H). Note that in the AMS the ion signal intensity is proportional to the mass of the aerosol species that created the signal, [see Canagaratna *et al.* (2007) for details]. The results for the 0.1% CH_4/N_2 photochemical aerosol are given in Fig. 1, and the aerosol is found to have a composition of 75% C, 16% N, and 9% H by mass. Based on the average AMS uncertainty of 20% reported by Aiken *et al.* (2007) for the N/C determination, we arrive at an estimate for the contribution of nitrogen to the aerosol mass of 16 ± 3%. This composition roughly corresponds to an "average" formula of $C_{11}H_{16}N_2$, a metric that is useful for comparisons to other analyses of laboratory-produced CH_4/N_2 haze analogs (*e.g.,* Imanaka *et al.,* 2004). Most notably, the atomic N/C ratio of 0.18 for our aerosol is lower than the values of 0.4–0.8 reported for aerosol produced by irradiation at lower wavelengths, whose higher photon energies facilitate a greater N_2 dissociation rate (Imanaka and Smith, 2010). N/C ratios for Titan-like hazes formed in various types of discharges vary considerably from 0.1 to 0.8 (Imanaka *et al.,* 2004).

Additional understanding of the chemical nature of the aerosol can be obtained by examining the series of ion peaks identified in the spectrum, rather than just interpreting the bulk elemental formula. The mass spectrum given in Fig. 1 displays the skeletal formulas (*i.e.,* without H atoms) derived from the high-resolution analysis for each of the groups of peaks on the "picket fence" pattern in the mass spectrum. Each peak at an integer *m/z* value represents that sum of ion signals from molecular fragments that have the skeletal formulas indicated above that group of peaks. For example, at *m/z* 55 there are possible contributions from $C_4H_7^+$, $C_3NH_5^+$, $C_2N_2H_3^+$, and CN_3H^+. The peak at *m/z* 56 contains contributions from ions with an additional hydrogen atom, namely, $C_4H_8^+$, $C_3NH_6^+$, $C_2N_2H_4^+$, and $CN_3H_2^+$. The hydrocarbon fragments C_1–C_7 are represented in the full mass

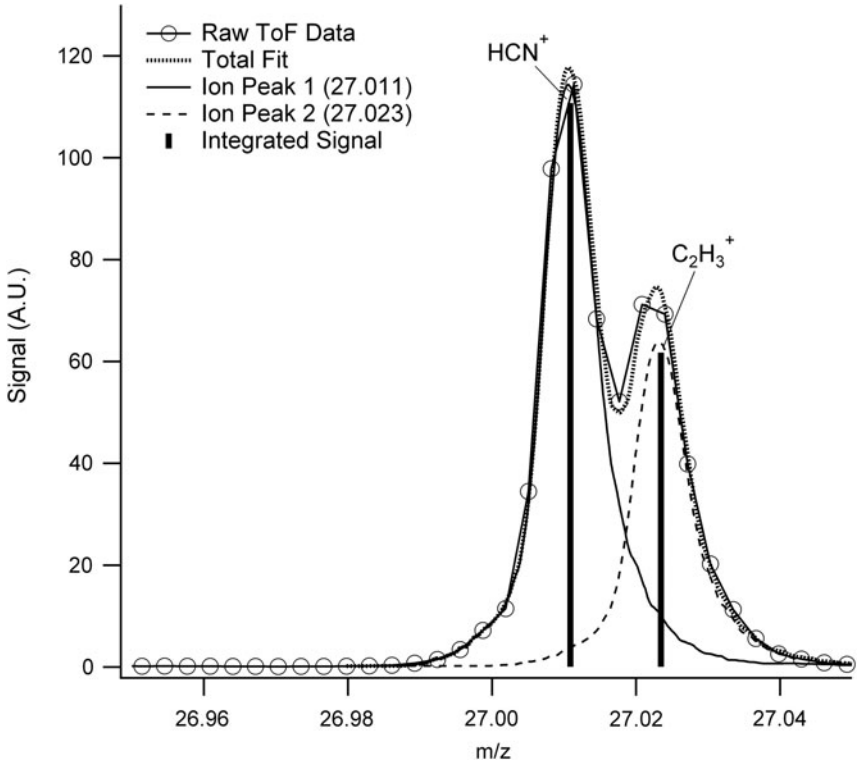

FIG. 2. The raw time-of-flight (ToF) mass spectrum is fit to quantify the ion contributions to the signal. The fitting algorithm determines the peak area to quantify the contribution from each ion and derive the elemental analysis (Aiken *et al.,* 2008). The comparison between the raw data and the total fit provide an indication of the goodness of fit. For *m/z* 27, the photochemical aerosol arising from a 0.1% CH_4/99.9% N_2 atmosphere shows peaks at *m/z* values of 27.011 and 27.023 which are most likely due to ions HCN^+ and $C_2H_3^+$, respectively. A.U., arbitrary units.

range shown. Nitrogenated organic species are represented by ions with N_1–N_3 in this mass range, but most (89% of C_xN_y mass) of the ion signal arises from fragments with one N atom. The bars in the mass spectrum are shaded to indicate the contributions of each element to the mass concentration represented by all ions at that integer *m/z*. It can be seen that with a few exceptions (aromatic-dominated *m/z* 77, $C_6H_5^+$ and *m/z* 91, $C_7H_7^+$) almost all the nominal *m/z* values contain a contribution from N. A closer look at the location of the center of each fragmentation packet reveals that the fragment masses skew toward unsaturated organics such as alkenes and nitriles (*m/z* 40–41, 54–55, 68–69, 82–83) and away from alkanes and amines (*m/z* 43–44, 57–58, 71–72, 84–85) (McLafferty and Turecek, 1993). This preference for unsaturated organics is consistent with inferences of unsaturated neutral molecules and ions high in Titan's atmosphere based on preface with the Cassini Ion and Neutral Mass Spectrometer observations (Vuitton *et al.,* 2007).

The photochemistry experiments discussed above were repeated by varying the N_2 concentration, as detailed in the Materials and Methods section. The results from this study are two-fold; both the proportion of N in the aerosol and the overall aerosol signal appear to be influenced by the N_2 concentration. Evidence of the latter effect can be observed in Fig. 3, wherein the aerosol spectra from experiments in which 0.1% CH_4 was used in different Ar/N_2 mixtures are compared. The spectra are scaled so that the mass loading of the most intense peak, which is at *m/z* 27 in the top panel, is 100. This scaling highlights the approximately 100-fold decrease in signal when CH_4 is photolyzed in pure Ar as compared to pure N_2. An experiment performed with 0.1% CH_4 in He (not shown) had similarly low aerosol yield as compared to the Ar results. The low particle yield in Ar is consistent with previous results reported by Bar-Nun and Podolak (1979), in which no condensed phase was observed after hours of irradiation of the same gas mixture by the same FUV wavelength range. Adamkovics and Boering (2003) saw aerosol production from CH_4-only irradiation with the same FUV source, but the CH_4 pressure, static chamber, and particle detection methods used were dissimilar enough from our experiments that it is not possible to compare their aerosol production rates to ours either with or without N_2. From Fig. 3, it is evident that there is a significant leap in aerosol production as even a small amount of N_2 is included in the reaction cell, which is demonstrated by the differences between the lower two panels (0% N_2 vs. 0.1% N_2). The difference in the spectra indicates a change in the number and abundance of mass peaks, which implies an increase in organic production. These results suggest not only that N_2 *can* be involved in the molecular structure of the organic aerosol but also that it *must* be involved for significant production of aerosol to occur, at least under our experimental conditions.

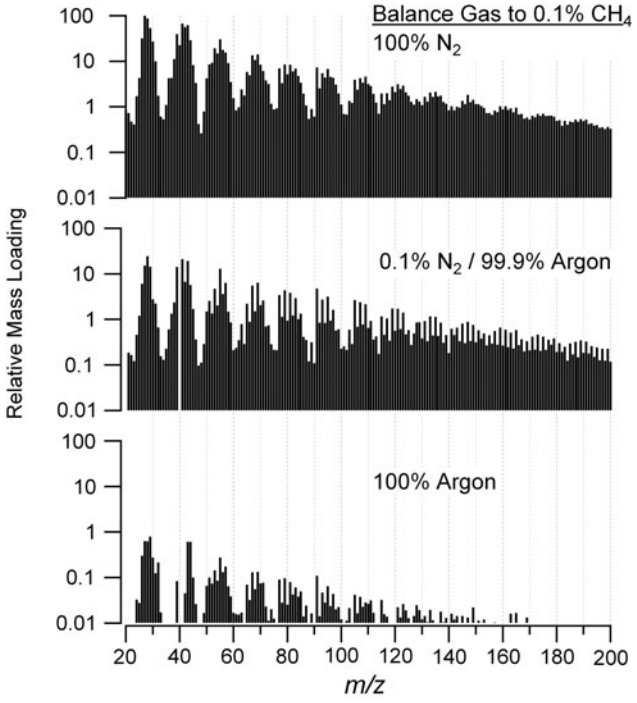

FIG. 3. Averaged aerosol mass spectra show the effect of N_2 concentration on the aerosol composition and relative mass production rate. The signals for the gases N_2 and Ar have been subtracted from the spectra.

The exact mechanism for the inclusion of nitrogen in the particles is unclear. At the experimental temperature, it is extremely unlikely that N_2 would be adsorbed onto the surface of the aerosols or trapped at sufficient mass quantities (>10%) to account for the observed nitrogen content of the aerosol. Even if trapped, the N_2 molecules would diffuse quickly out of the nanometer-sized particles in the vacuum system of the HR-ToF-AMS during the 10 ms flight prior to vaporization (Snijder *et al.,* 1995). To investigate whether the nitrile production could be an artifact due to species formation within the ionization region of the AMS, an additional control experiment was performed in which the CH_4/Ar mixture was photolyzed in the reaction cell and N_2 gas was added to the aerosol flow downstream, before the inlet of the HR-ToF-AMS. In this control, the HCN^+ peak at *m/z* 27.01 was absent, and the average mass spectrum did not vary as the proportion of N_2 introduced downstream was varied. These results indicate that the nitrogen-incorporating chemistry is a result of photolysis within the cell.

Select nominal *m/z* regions—26, 27, 29, 53, and 77—are expanded into high-resolution view in Fig. 4. Here, the traces and peak identifications of several N_2/Ar combinations are compared. The integer *m/z* 26, 27, and 29 were chosen since these are the peaks in the fragmentation packet with the highest relative signal and serve as tracers for the relationship between nitrile (CN^+, HCN^+) and hydrocarbon ($C_2H_2^+$, $C_2H_3^+$) production. As the proportion of N_2 is decreased, the relative contribution of the nitrile fragments also decreases. At nominal *m/z* 29, we also observe an example of a peak that cannot be uniquely identified at our resolution. Here, the signal at *m/z* 29.003 could be due to two possible ions, marked with asterisks: $N^{15}N^+$ (29.00318) and CHO^+ (29.00274). By comparing the aerosol product spectrum to the spectrum of the gas mixture acquired prior to the lamp ignition, we were able to estimate that approximately 15% of that peak in the 100% N_2 experiment is due to the gas-phase nitrogen isotope signal, and the remainder is likely from the contribution of the CHO^+ fragment. This proportion of $N^{15}N^+$ is smaller for the other two experiments shown in Fig 4. The CHO^+ fragment may be evidence of some oxygen contamination in our system from residual H_2O. Fortunately, there are few occurrences of oxygen contamination in our results.

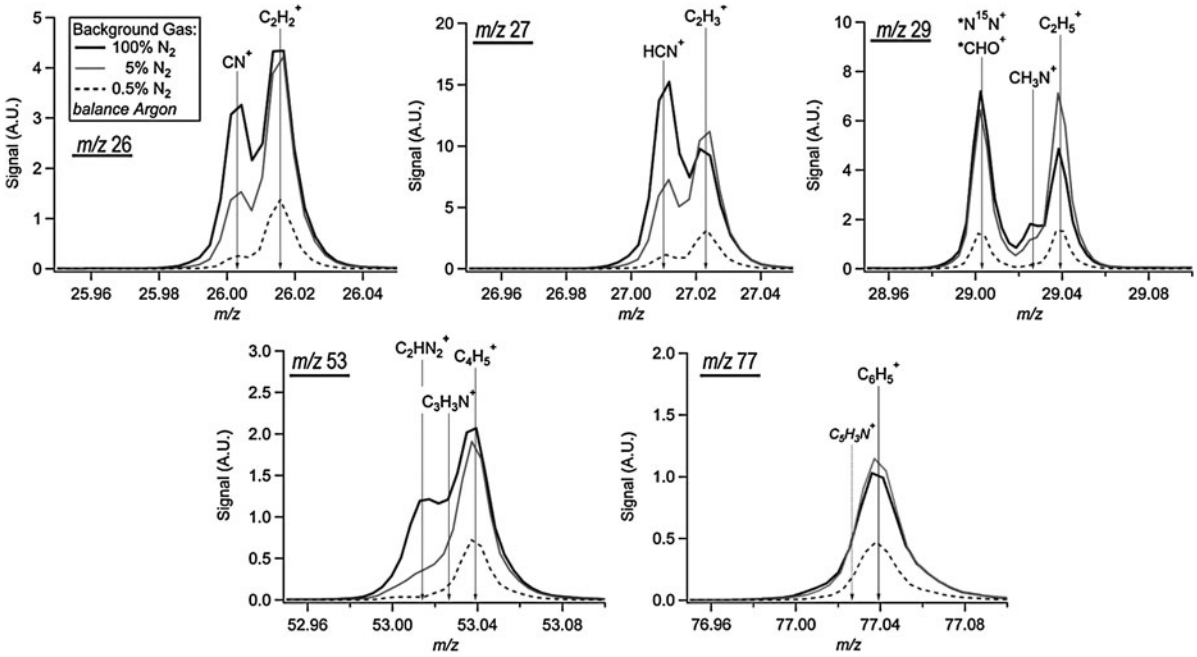

FIG. 4. High-resolution ion signal for key fragment ions observed in the aerosol spectrum from 0.1% CH_4 photolysis. The relative contribution to ion peaks as a function of background gas mixture (N_2:Ar) is demonstrated by the solid and dashed traces. The peak at *m/z* 29.003 (the ion identifications marked with *) may be due to either of two molecular fragments which are indistinguishable at the instrument resolution. Ion signal is shown in arbitrary units, and traces have been normalized so that the height of the largest ion is similar in each plot.

The high-resolution view of nominal *m/z* 53 in Fig. 4 shows the multi-peak results typical at higher *m/z*, where the ion population contains several ions in the 100% N_2 experiments but only one dominant ion when Ar is the primary background gas. The $C_xH_yN_z^+$ fragments are clearly present at almost all of the *m/z* values in the 100% N_2 spectrum except when there is an aromatic ion (*m/z* 77, 91). At these *m/z* values, the signal from the aromatic ion is sufficiently greater than those of surrounding ions that it is difficult to resolve the contribution from any possible N-containing ions that may be present. This difficulty is demonstrated in Fig. 4. At all N_2 concentrations, the peak at *m/z* 77.039 is identified as the phenyl ion $C_6H_5^+$. However, as shown in the figure, the N-containing ion $C_5H_3N^+$ might be present.

As can be seen in Fig. 4, at *m/z* 27 there is a definitive change in the ratio between the nitrile and hydrocarbon contributions as the N_2 concentration is decreased. This peak has the highest signal intensity in the observed mass spectra, represents a substantial fraction of the total aerosol mass, and does not have any interference from N_2 gas. The ratio of these two fragments at *m/z* 27 was therefore chosen as a marker for the degree of nitrogen incorporation into the organic aerosol chemical structure. The ratio is shown plotted as a function of the percent N_2 in the gas mixture (balance Ar) in Fig. 5. Figure 5 also contains a plot of the atomic N/C ratio as a function of N_2 percentage. There is some variability in these observed ratios from experiment to experiment, but the overall trend with N_2 concentration is clear. These data show that a shift in chemical composition occurs between the all-hydrocarbon products generated in Ar and the nitrogenated aerosol formed in N_2-containing mixtures. Above a N_2 concentration of 10%, the contribution of the nitrile fragment to the nominal *m/z* 27 dominates that from the hydrocarbon fragment.

4. Photochemical Formation of CN Bond

The formation of HCN from the irradiation of CH_4 and N_2 mixtures at wavelengths >125 nm was first reported by Dodonova (1966), with an approximate yield of 10^{-5} HCN molecules per photon (Chang *et al.*, 1979). This result was derived by using a very specific detection technique sensitive only to gas-phase HCN, with corroboration from measurement of trapped gases with a mass spectrometer. Another study (Scattergood *et al.*, 1989) in which broadband light from a discharge with a lower transmission edge at 115 nm was used also reported gaseous HCN production with a yield of approximately 10^{14} molecules per joule (equivalent to 10^{-4} HCN molecules per Ly-α photon). Neither of these studies proposed a mechanism for HCN formation (Scattergood *et al.*, 1989). Using the compositional information retrieved from the HR-ToF-AMS, the total aerosol mass production rates and photon flux reported in our previous work, and an assumption that each nitrogen atom within the aerosol is bonded to a carbon atom (a reasonable assumption given the fragment ions observed), we calculated an approximate yield of 10^{-3} C-N linkages generated per photon within our cell. This value is 2 orders of magnitude greater than the HCN yield reported by Dodonova (1966) and one order greater than Scattergood *et al.* (1989), which is not surprising given the much broader detection capability of our method. With the HR-ToF-AMS, we observed a myriad of particle-phase

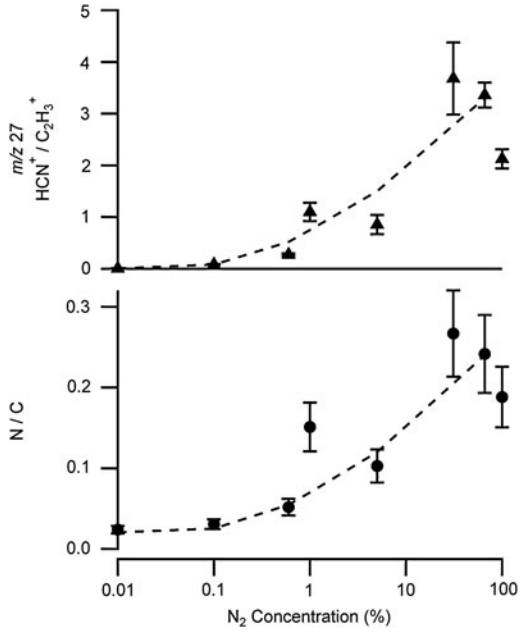

FIG. 5. Plots of the ratio of the contribution of the nitrile (HCN^+) to the hydrocarbon ($C_2H_3^+$) ion fragments for *m/z* 27 signal (top panel) and the N/C ratio in the aerosol spectra (bottom panel) as a function of the proportion of N_2 in the background gas during photolysis of 0.1% CH_4. Argon was used as the balance gas during these experiments, and the total pressure in the reaction cell was held constant at 600 torr. Each point represents an averaged value for one experiment. For the *m/z* 27 peak height data in the top panel the error bars show the standard deviation to indicate the variability within each experiment. For the N/C data in the bottom panel the error bars represent the 20% error in this ratio cited for the instrument (Aiken *et al.*, 2007). The dashed lines are included as a guide to the eye.

compounds with –CN groups, which may have been produced with a higher yield than HCN gas.

Interestingly, when other workers in the 1970s and early 1980s attempted to repeat the results of Dodonova (1966) but failed to produce nitriles or N-containing organics in the UV (Ferris and Chen, 1975; Chang *et al.*, 1979; Bossard *et al.*, 1982; Raulin *et al.*, 1982), Bossard *et al.* (1982) concluded that "UV light is not able to produce nitriles from CH_4-N_2 mixtures" and "UV light is not an efficient source for producing unsaturated carbon chains." The results presented herein clearly contradict those conclusions. It is difficult to directly compare the results from these previous publications to ours due to variations in experimental conditions (pressure, temperature) and measurement techniques. Table 1, adapted from Raulin *et al.* (1982), reviews the previous findings alongside the results presented in this work. Notably, the observations summarized in Table 1 show that, with the exception of the studies by Dodonova (1966) and Scattergood *et al.* (1989), the other works were performed by using line sources rather than continuum sources such as the one used in our study. While the absorption cross sections are known in the continuum, there has been very little work done on the branching ratio of CH_4 dissociation when using continuum radiation because the EUV solar flux is dominated by Ly-α. However, a compilation published by Huebner *et al.* (1992) shows that across the continuum range the formation rates of CH_4 photolysis products CH_3, CH_2, and CH do vary relative to each other, which indicates that there is a bias toward or away from particular radical products when a line source is used rather than a continuum. Additionally, two of the studies reported in Table 1 were performed by using wavelengths above the threshold for CH formation of 137 nm. Imanaka and Smith (2007) explored the formation of gas-phase species at EUV and FUV wavelengths and found the production of larger hydrocarbons (C_7–C_8) absent in the FUV, but they were unable to distinguish nitrogen incorporation in the organic species and did not measure the composition of the particle phase. Hodyss *et al.* (2011) observed –CN formation in water ice from CH_4/N_2 photolysis at similar wavelengths. Although occurring within different matrices, this is further evidence that a mechanism to cleave N_2 at $\lambda > 100$ nm via CH_4 photolysis needs to be considered. Hodyss *et al.* (2011) suggested that generation of CH radicals may initiate the process, and we will explore this possibility in more detail below.

Despite early experimental results on HCN formation, there are no proposed mechanisms for nitrogen activation at FUV wavelengths that have been put forward in the literature. The N-N triple bond in N_2 is among the strongest of chemical bonds, and direct photolysis of N_2 does not take place unless the photons have wavelengths shorter than 110 nm, as shown in Fig. 6. Although the bond energy determined thermodynamically is 9.76 eV (compared to 10.2 eV of Ly-α photon), the absorption cross section of N_2 is negligible in this region of the spectrum (*e.g.*, see Huebner *et al.*, 1992). By far, the most extensive chemical modeling of organic chemistry within a CH_4/N_2 atmosphere addresses the processes on Titan, which includes an array of nitrile products. In all cases, nitrile chemistry is initiated via the

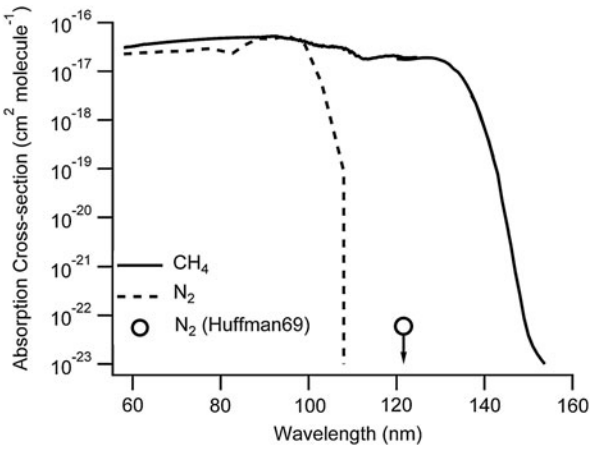

FIG. 6. The absorption cross sections for CH_4 (Mount *et al.*, 1977; Kameta *et al.*, 2002; Chen and Wu, 2004) and N_2 (Chan *et al.*, 1993) show that direct dissociation of N_2 is not expected in the FUV. The vertical dashed line indicates the lower limit of our lamp emission. Huffman (1969) does report a cross-section measurement at Ly-α of 6×10^{-23} cm^2 (open circle) but provides this only as an upper bound based on the detection limit of the instrumentation. As demonstrated by the graph, even with this upper limit the absorption of N_2 is not competitive as compared to CH_4, and direct dissociation cannot explain the high percentage of N_2 incorporated into the aerosol material.

dissociation or ionization of N_2 by energetic electrons within Saturn's magnetosphere or, more significantly, with solar EUV (Yung *et al.*, 1984; Wilson and Atreya, 2004; Lavvas *et al.*, 2011). Theoretical studies focused on Ly-α photolysis have only explored hydrocarbon chemistry (Wilson and Atreya, 2000).

It thus appears that there is a mechanism missing from the literature, which is needed to explain the chemical activation of N_2 within our photochemical cell. One possibility is indirect N-N cleavage, which has been proposed to explain the formation of "prompt" NO in the combustion of CH_4 in air, as discovered by Fenimore (1971). The two-step process begins with photolysis of CH_4 (*e.g.*, by Ly-α) to produce the CH radical (see, *e.g.*, Yung *et al.*, 1984; Hebrard *et al.*, 2006; Lodriguito *et al.*, 2009) followed by reaction to form HCN:

$$CH_4 + h\nu \rightarrow CH + H_2 + H \quad \text{(R1)}$$

$$CH + N_2 \rightarrow HCN + N \quad \text{(R2)}$$

However, Reaction R2 is spin-forbidden, as the ground states of CH and N are $^2\Pi$ and ^4S, respectively. Consequently, the reaction has large activation energy. The theoretical rate coefficient that fits most of the laboratory measurements between 1500 and 4000 K (Miller and Walch, 1997) is $k = 3.68\times10^{7}\, T^{1.42} \exp(-20723/RT)$ cm^3 mol^{-1} s^{-1}. If we apply this formula at room temperature, as in our reaction cell, the rate coefficient is 5×10^{-17} cm^3 s^{-1}. This value compares well to those presented by Becker *et al.* (1996) (*i.e.*, Table IV), where the authors estimated a rate coefficient for R2 at the lowest temperature (572 K) and lowest pressure (20 torr) to be 2.9×10^{-20} cm^3 s^{-1}. These results led Becker *et al.* (1996) and other groups to determine that the influence of this bimolecular reaction on the $CH + N_2$ *k*-values is negligible. In this case reaction of CH with CH_4,

$$CH + CH_4 \rightarrow C_2H_4 + H \quad \text{(R3)}$$

with a rate coefficient around 10^{-10} cm^3 s^{-1} will dominate.

Alternatively, the reaction between CH and N_2 via a termolecular process can lead to the formation of the diazomethyl radical HCN_2 and its isomer the HNCN radical, which is more stable by 34.4 kcal/mol (Tao *et al.*, 1994; Clifford *et al.*, 1998; Moskaleva *et al.*, 2000; Berman *et al.*, 2007):

$$CH + N_2 + M \rightarrow HCN_2 \quad \Delta H = -28.2 \text{ kcal/mol} \quad \text{(R4a)}$$

$$\rightarrow HNCN \quad \Delta H = -62.6 \text{ kcal/mol} \quad \text{(R4b)}$$

albeit with unknown branching ratios. The addition reaction is apparently fast, even at low temperatures (Le Picard and Canosa, 1998; Le Picard *et al.*, 1998), which suggests that the reaction has no kinetic barrier. The third-order rate constant was found to be $k_0 = (5.7\pm0.30)\times10^{-30}$ cm^6 s^{-1} at 53 K (Le Picard and Canosa, 1998), with similar values at room temperature (Becker *et al.*, 1996; Brownsword *et al.*, 1996).

The fate of HCN_2 is most likely reaction with H:

$$H + HCN_2 \rightarrow HCN + NH \quad \Delta H = -47.4 \text{ kcal/mol} \quad \text{(R5a)}$$

$$\rightarrow H_2 + CN_2 \quad \Delta H = -25.2 \text{ kcal/mol} \quad \text{(R5b)}$$

$$\rightarrow CH_2 + N_2 \quad \Delta H = -70.9 \text{ kcal/mol} \quad \text{(R5c)}$$

$$H + HNCN \rightarrow HCN + NH \quad \Delta H = -13.0 \text{ kcal/mol} \quad \text{(R5d)}$$

$$\rightarrow H_2 + NCN \quad \Delta H = 9.2 \text{ kcal/mol} \quad \text{(R5e)}$$

$$\rightarrow CH_2 + N_2 \quad \Delta H = -36.5 \text{ kcal/mol} \quad \text{(R5f)}$$

Unfortunately, the branching ratios for the above reactions are completely unknown. Note that pathways (a), (d), and (e) result in the breaking of a N-N bond and the formation of a C-N bond, although (e) is slightly endothermic. Photolysis of HCN_2 may also be possible but with unknown cross sections or products (Faulhaber *et al.*, 2006). The only atmospheric model that has studied the formation of HCN from $CH + N_2$ is that of Krasnopolsky and Cruikshank (1999). They estimated the HCN yield (*Y*) relative to total photolysis of CH_4 to be about 1×10^{-7} for the atmosphere of Pluto, which suggests that this pathway has a small impact in a planetary atmosphere. In the laboratory experiments described herein involving irradiation of a mixture of CH_4 and N_2 by a deuterium lamp, CH radicals were readily produced, and the third-body concentration was very large. If *Y* is defined as $f_1\times f_2\times f_3\times f_4$, where f_1 = branching ratio for producing CH in CH_4 photolysis, f_2 = fraction of CH that reacts with N_2 to form HCN_2 and HNCN, f_3 = fraction of HCN_2 and HNCN that reacts with H, and f_4 = fraction of above reaction that results in the formation of HCN or a CN bond, then the upper limit for *Y* would be equivalent to f_1, which ranges in the literature from 7% to 51% (Wilson and Atreya, 2000). Yet, given all the unknown parameters, it is difficult to assess whether this reaction scheme is the likely explanation for the formation of –CN bonds and the high nitrogen incorporation observed in the organic aerosol in our experiments.

Likewise, we have explored the possibility of radiative association reactions of $CH_3^+ + N_2 \rightarrow CH_3N_2^+$ as a mechanism for activation of nitrogen within the photolysis cell (Holtz and Beauchamp, 1971). At Ly-α, CH_3^+ can be formed from the photoionization of CH_3 radicals. If reaction of CH_3^+ with N_2 is competitive with reaction with CH_4, this may be a source of activated N_2. Smith and Adams (1978) reported a rate coefficient of 5×10^{-29} cm^3 s^{-1} for the formation of $CH_3N_2^+$ at conditions relevant to the experimental reaction cell, and this is supported by calculations of Phillips (1990). A rate coefficient for $CH_3^+ + CH_4$ is given as 1×10^{-9} cm^3 s^{-1} in Vuitton *et al.* (2008). Thus in our reaction cell with 0.1% CH_4 in N_2, the reaction with CH_4 will likely dominate. The production of $CH_3N_2^+$ may therefore be too low to substantiate the high observed nitrogen content in the laboratory aerosol. Also problematic is that there is not a known pathway to HCN or –CN groups from the $CH_3N_2^+$ ion.

The excited state $CH(a^4\Sigma)$ is 0.74 eV above the ground state $CH(X^2\Pi)$ and can drive the spin-allowed exoergic reaction:

$$CH(a^4\Sigma) + N_2(X^1\Sigma) \rightarrow HCN(X^1\Sigma) + N(^4S) \quad \text{(R6)}$$

However, only an upper limit of 6×10^{-14} cm^3 s^{-1} has been measured for this reaction (Hou and Bayes, 1993). As the reaction between $CH(a^4\Sigma)$ and CH_4 is also slow (Hou and Bayes, 1993), it is possible that there is a path for direct formation of HCN by the above reaction in the laboratory and the atmosphere.

Surveys of currently known experimental pathways have not yielded a "smoking gun" mechanism to explain the results reported in this work. Clearly, further work (experimental and theoretical) is needed to illuminate this problem and provide the missing mechanism. Future studies of these processes at lower pressures would be highly desirable to determine whether the termolecular process proposed here

may be the source of the unexpected nitrogen incorporation. Likewise, a systematic exploration of the wavelength dependence would be enlightening.

5. Implications

The formation of HCN or nitrile-rich materials is of great interest with regard to multiple planetary bodies within the Solar System because of the strong spectral features and prebiological potential of these types of molecules (Matthews, 1992). Thus, it is important to understand the complete range of formation conditions given the wide array of radiation and compositional constraints of different planetary environments. For early Earth, there has long been a question as to how Miller-Urey–type prebiotic chemistry with N-containing organics may have taken place without a large abundance of NH_3 in the atmosphere (Toupance *et al.*, 1977; Pavlov *et al.*, 2001). FUV light is the presumed preeminent energy source on early Earth, and these results have significant implications for understanding the chemical nature of a globally available organics source (Trainer *et al.*, 2006; Wolf and Toon, 2010). The results presented here are complementary to recent modeling of enhanced HCN formation on an early Earth with abundant CH_4, and as suggested by Tian *et al.* (2011), we have shown that you can get significant –CN incorporation in the haze particles, which may later deposit into oceans for further reaction. Further work regarding the impact of CO_2 and H_2 on the nitrogen chemistry needs to be completed (Tian *et al.*, 2005; Haqq-Misra *et al.*, 2008).

Whether FUV production of reactive nitrogen has relevance for Titan is dependent on whether the majority of chemical production of aerosol takes place in the stratosphere or the primary energy input that drives organic chemistry and haze formation occurs higher in the thermosphere and ionosphere due to photolysis at EUV wavelengths, as some have suggested (Lavvas *et al.*, 2009, 2011). It is also dependent on the chemical mechanism responsible for the N_2 activation. Figure 7 demonstrates why the reaction pathways discussed in the previous section (R4 and R5) may not be relevant on Titan. On Titan, where CH_4 is abundant, reactions of $CH + CH_4$ dominate in haze-forming regions. However, the reactions with N_2 could be relevant for early Earth. The formation of nitriles from CH via reaction with N_2 can only take place in regions where $k_c[CH_4] < k_n[N_2][M]$. In such regions, the pressure is great enough that the N_2 molecules are plentiful relative to CH_4 so that reaction of CH with N_2 can compete. There was a lower concentration of CH_4 on early Earth, and the haze formed at a lower altitude (*i.e.*, higher pressure), both of which would have made the reaction of CH with N_2 more competitive (Wolf and Toon, 2010). Figure 7 shows the relative lifetimes of CH radical for an early Earth CH_4 mixing ratio of 1000 ppmv and indicates that in the haze formation region this reaction mechanism could have contributed to nitrogenated organics forming in the haze on early Earth. However, other mechanisms are possible that could have had different dependences on altitude. CH_4/N_2 photochemistry also holds interest for the study of Neptune's moon Triton (McDonald *et al.*, 1994).

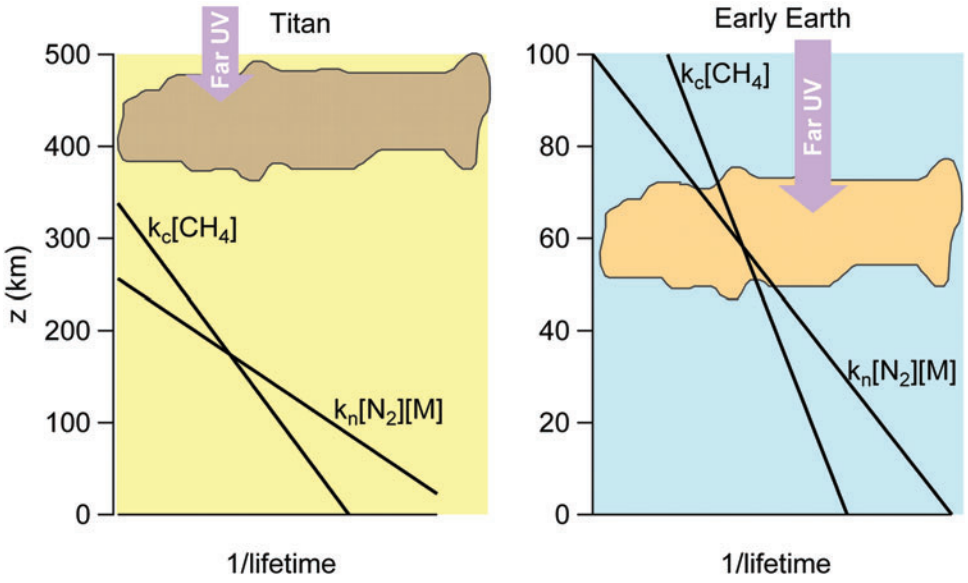

FIG. 7. The lifetime of the CH radical, produced via CH_4 photolysis, is evaluated for both Titan and early Earth for two different reaction pathways. Curves labeled $k_c[CH_4]$ represent the lifetime with respect to the reaction $CH + CH_4$, with the second-order rate constant $k_c = 10^{-10}$ cm^3 molecule^{-1} s^{-1} (Yung *et al.*, 1984). Curves labeled $k_n[N_2][M]$ represent the lifetime with respect to the reaction $CH + N_2 + M$ (R3), with the third-order rate constant $k_n = 5.7 \times 10^{-30}$ cm^6 molecule^{-2} s^{-1} (Le Picard and Canosa, 1998). A concentration of approximately 2% CH_4 is assumed for Titan, and 1000 ppmv for early Earth. The curves cross at the transition where the pressure is great enough that the number density of N_2 molecules outnumbers the CH_4 molecules by enough to successfully compete for reaction with CH. If this transition occurs above or within the haze formation region—shown on the plot with the cloud cartoon—then the formation of nitriles can influence the chemical composition of the haze. Color images available online at www.liebertonline.com/ast

Interestingly, FUV nitrogen dissociation may have implications for our assessment of the extent of prebiotic chemistry in planets beyond our solar system. Due to their high abundance in the Galaxy and long-term stability, low-mass M stars (or M dwarfs) are often considered targets to search for terrestrial planets in the habitable zone (Scalo *et al.,* 2007). Many researchers have evaluated the possibility that a planet like Earth could remain habitable in orbit around an M dwarf if the effects of the strong stellar flares (Segura *et al.,* 2010) and lower insolation (Joshi *et al.,* 1997) were mitigated in some way. An alternate side of this discussion is whether a planet like early Earth would have sufficiently advanced prebiotic chemistry for life to arise in the first place (Buccino *et al.,* 2006). The M dwarf spectrum is shifted longward as compared to our sun and has a significantly decreased UV flux (Segura *et al.,* 2005). Like the case of early Earth discussed above, formation of C-N bonds would occur in an environment without strong EUV flux. Buccino *et al.* (2007) determined that there was not enough UV flux at planets around quiet M dwarf stars to promote the prebiotic synthesis necessary to initiate life but did not specify chemical reactions of interest or take into account the wavelengths of light needed for CH_4 dissociation. Stars with moderate to high flare activity will experience bursts of strong UV flux that may be sufficient for this type of synthesis (Segura *et al.,* 2010). Although spectra of M dwarfs provided in the literature do not include radiation shortward of 100 nm, presumably the FUV flux is greater than the EUV radiation otherwise required to break N_2 bonds (Segura *et al.,* 2007; Walkowicz *et al.,* 2008). As shown in this paper, photolysis of even trace amounts of CH_4 and N_2 in an anoxic atmosphere can cleave the N_2 bond and produce nitrogen-containing organic molecules without the presence of EUV.

Ultimately, the unanticipated nitrogen chemistry signals a missing reaction mechanism for the activation of N_2 via CH_4 photolysis at wavelengths greater than 115 nm. The observed level of nitrogen incorporation, up to 16% by mass with a N/C of approximately 0.18, was not predicted by current models of CH_4/N_2 chemistry at these wavelengths. Although possible mechanisms have been proposed here, there is not enough data currently available to assess these as the source of the nitrile groups in the aerosol. Thus, as indicated by the unexpected nature of these results, a re-evaluation of the photochemical reaction schemes in this wavelength range and further investigation into the nature of the secondary reactions that lead to the chemical activation of N_2 are clearly needed.

Acknowledgments

M.G.T. thanks R. Lessard, C. Hasenkopf, and D. Day for help with control experiments. Y.L.Y. thanks K. Bayes, S. Sander, and W. DeMore for discussion of the kinetics of CH reactions. This work was funded by NASA grants NNX07AV55G, NNX11AD82G, and NNX08AG93G. The development of the HR-ToF-AMS and its analysis software was partially funded by NSF ATM-0449815 and NOAA NA08OAR4310565. Y.L.Y. was supported by NASA grant NX09AB72G to the California Institute of Technology.

Disclosure Statement

No competing financial interests exist.

Abbreviations

AMS, aerosol mass spectrometer; EUV, extreme ultraviolet; FUV, far ultraviolet; HR-ToF-AMS, high-resolution time-of-flight aerosol mass spectrometer; *m/z*, mass-to-charge ratio; Q-AMS, quadrupole aerosol mass spectrometer.

References

Adamkovics, M. and Boering, K.A. (2003) Photochemical formation rates of organic aerosols through time-resolved *in situ* laboratory measurements. *J Geophys Res* 108:5092–5105.

Aiken, A.C., DeCarlo, P.F., and Jimenez, J.L. (2007) Elemental analysis of organic species with electron ionization high-resolution mass spectrometry. *Anal Chem* 79:8350–8358.

Aiken, A.C., Decarlo, P.F., Kroll, J.H., Worsnop, D.R., Huffman, J.A., Docherty, K.S., Ulbrich, I.M., Mohr, C., Kimmel, J.R., Sueper, D., Sun, Y., Zhang, Q., Trimborn, A., Northway, M., Ziemann, P.J., Canagaratna, M.R., Onasch, T.B., Alfarra, M.R., Prevot, A.S.H., Dommen, J., Duplissy, J., Metzger, A., Baltensperger, U., and Jimenez, J.L. (2008) O/C and OM/OC ratios of primary, secondary, and ambient organic aerosols with high-resolution time-of-flight aerosol mass spectrometry. *Environ Sci Technol* 42:4478–4485.

Bar-Nun, A. and Podolak, M. (1979) Photochemistry of hydrocarbons in Titan's atmosphere. *Icarus* 38:115–122.

Becker, K.H., Geiger, H., and Wiesen, P. (1996) Kinetics of the reaction $CH + N_2$ [M] ® products in the range 10–620 torr and 298–1059 K. *International Journal of Chemical Kinetics* 28: 115–123.

Berman, M.R., Tsuchiya, T., Gregusova, A., Perera, S.A., and Bartlett, R.J. (2007) HNNC radical and its role in the $CH + N_2$ reaction. *J Phys Chem A* 111:6894–6899.

Bossard, A.R., Raulin, F., Mourey, D., and Toupance, G. (1982) Organic synthesis from reducing models of the atmosphere of the primitive Earth with UV-light and electric discharges. *J Mol Evol* 18:173–178.

Brownsword, R.A., Herbert, L.B., Smith, I.W.M., and Stewart, D.W.A. (1996) Pressure and temperature dependence of the rate constants for the association reactions of CH radicals with CO and N_2 between 202 and 584 K. *Journal of the Chemical Society, Faraday Transactions* 92:1087–1094.

Buccino, A.P., Lemarchand, G.A., and Mauas, P.J.D. (2006) Ultraviolet radiation constraints around the circumstellar habitable zones. *Icarus* 183:491–503.

Buccino, A.P., Lemarchand, G.A., and Mauas, P.J.D. (2007) UV habitable zones around M stars. *Icarus* 192:582–587.

Canagaratna, M.R., Jayne, J.T., Jimenez, J.L., Allan, J.D., Alfarra, M.R., Zhang, Q., Onasch, T.B., Drewnick, F., Coe, H., Middlebrook, A., Delia, A., Williams, L.R., Trimborn, A.M., Northway, M.J., DeCarlo, P.F., Kolb, C.E., Davidovits, P., and Worsnop, D.R. (2007) Chemical and microphysical characterization of ambient aerosols with the aerodyne aerosol mass spectrometer. *Mass Spectrom Rev* 26:185–222.

Chan, W.F., Cooper, G., Sodhi, R.N.S., and Brion, C.E. (1993) Absolute optical oscillator strengths for discrete and continuum photoabsorption of molecular nitrogen (11–200 eV). *Chem Phys* 170:81–97.

Chang, S., Scattergood, T., Aronowitz, S., and Flores, J. (1979) Organic chemistry on Titan. *Rev Geophys* 17:1923–1933.

Chen, F.Z. and Wu, C.Y.R. (2004) Temperature-dependent photoabsorption cross sections in the VUV-UV region. I. Methane and ethane. *J Quant Spectrosc Radiat Transf* 85:195–209.

Chhabra, P.S., Flagan, R.C., and Seinfeld, J.H. (2010) Elemental analysis of chamber organic aerosol using an aerodyne high-

resolution aerosol mass spectrometer. *Atmos Chem Phys* 10:4111–4131.

Clarke, D.W. and Ferris, J.P. (1997) Titan haze: structure and properties of cyanoacetylene and cyanoacetylene-acetylene photopolymers. *Icarus* 127:158–172.

Clifford, E.P., Wenthold, P.G., Lineberger, W.C., Petersson, G.A., Broadus, K.M., Kass, S.R., Kato, S., DePuy, C.H., Bierbaum, V.M., and Ellison, G.B. (1998) Properties of diazocarbene [CNN] and the diazomethyl radical [HCNN] via ion chemistry and spectroscopy. *J Phys Chem A* 102:7100–7112.

Coustenis, A., Achterberg, R.K., Conrath, B.J., Jennings, D.E., Marten, A., Gautier, D., Nixon, C.A., Flasar, F.M., Teanby, N.A., Bezard, B., Samuelson, R.E., Carlson, R.C., Lellouch, E., Bjoraker, G.L., Romani, P.N., Taylor, F.W., Irwin, P.G.J., Fouchet, T., Hubert, A., Orton, G.S., Kunde, V.G., Vinatier, S., Mondellini, J., Abbas, M.M., and Courtin, R. (2007) The composition of Titan's stratosphere from Cassini/CIRS mid-infrared spectra. *Icarus* 189:35–62.

DeCarlo, P.F., Kimmel, J.R., Trimborn, A., Northway, M.J., Jayne, J.T., Aiken, A.C., Gonin, M., Fuhrer, K., Horvath, T., Docherty, K.S., Worsnop, D.R., and Jimenez, J.L. (2006) Field-deployable, high-resolution, time-of-flight aerosol mass spectrometer. *Anal Chem* 78:8281–8289.

DeWitt, H.L., Trainer, M.G., Pavlov, A.A., Hasenkopf, C.A., Aiken, A.C., Jimenez, J.L., McKay, C.P., Toon, O.B., and Tolbert, M.A. (2009) Reduction in haze formation rate on prebiotic Earth in the presence of hydrogen. *Astrobiology* 9:447–453.

Dodonova, N.Y. (1966) Activation of nitrogen by vacuum ultraviolet radiation. *Russian J Phys Chem* 40:523–524.

Dzepina, K., Arey, J., Marr, L.C., Worsnop, D.R., Salcedo, D., Zhang, Q., Onasch, T.B., Molina, L.T., Molina, M.J., and Jimenez, J.L. (2007) Detection of particle-phase polycyclic aromatic hydrocarbons in Mexico City using an aerosol mass spectrometer. *Int J Mass Spectrom* 263:152–170.

Faulhaber, A.E., Gascooke, J.R., Hoops, A.A., and Neumark, D.M. (2006) Photodissociation dynamics of the HCNN radical. *J Chem Phys* 124:204303.

Fenimore, C.P. (1971) Formation of nitric oxide in premixed hydrocarbon flames. In *13th International Symposium on Combustion*, Salt Lake City, UT; pp 373–380.

Ferris, J.P. and Chen, C. T. (1975) Chemical evolution. XXVI. Photochemistry of methane, nitrogen, and water mixtures as a model for the atmosphere of the primitive Earth. *J Am Chem Soc* 97:2962–2967.

Haqq-Misra, J.D., Domagal-Goldman, S.D., Kasting, P.J., and Kasting, J.F. (2008) A revised, hazy methane greenhouse for the Archean Earth. *Astrobiology* 8:1127–1137.

Hasenkopf, C.A., Beaver, M.R., Trainer, M.G., Langley Dewitt, H., Freedman, M.A., Toon, O.B., McKay, C.P., and Tolbert, M.A. (2010) Optical properties of Titan and early Earth haze laboratory analogs in the mid-visible. *Icarus* 207:903–913.

Hebrard, E., Dobrijevic, M., Benilan, Y., and Raulin, F. (2006) Photochemical kinetics uncertainties in modeling Titan's atmosphere: a review. *Journal of Photochemistry and Photobiology C: Photochemistry Reviews* 7:211–230.

Hodyss, R., Howard, H.R., Johnson, P.V., Goguen, J.D., and Kanik, I. (2011) Formation of radical species in photolyzed CH_4:N_2 ices. *Icarus* 214:748–753.

Holtz, D. and Beauchamp, J. (1971) Nitrogen and carbon monoxide as nucleophilic reagants in gas phase displacement reactions: a novel means of nitrogen fixation. *Nature* 231:204–205.

Hou, Z.G. and Bayes, K.D. (1993) Rate constants for the reaction of $CH(a^4\Sigma)$ with NO, N_2, N_2O, CO, CO_2, and H_2O. *J Phys Chem* 97:1896–1900.

Huebner, W.F., Keady, J.J., and Lyon, S.P. (1992) Solar photo rates for planetary atmospheres and atmospheric pollutants. *Astrophys Space Sci* 195:1–294.

Huffman, R.E. (1969) Absorption cross-sections of atmospheric gases for use in aeronomy. *Can J Chem* 47:1823–1834.

Imanaka, H. and Smith, M.A. (2007) Role of photoionization in the formation of complex organic molecules in Titan's upper atmosphere. *Geophys Res Lett* 34, doi:10.1029/2006GL028317.

Imanaka, H. and Smith, M.A. (2010) Formation of nitrogenated organic aerosols in the Titan upper atmosphere. *Proc Natl Acad Sci USA* 107:12423–12428.

Imanaka, H., Khare, B.N., Elsila, J.E., Bakes, E.L.O., McKay, C.P., Cruikshank, D.P., Sugita, S., Matsui, T., and Zare, R.N. (2004) Laboratory experiments of Titan tholin formed in cold plasma at various pressures: implications for nitrogen-containing polycyclic aromatic compounds in Titan haze. *Icarus* 168: 344–366.

Joshi, M.M., Haberle, R.M., and Reynolds, R.T. (1997) Simulations of the atmospheres of synchronously rotating terrestrial planets orbiting M dwarfs: conditions for atmospheric collapse and the implications for habitability. *Icarus* 129:450–465.

Kameta, K., Kouchi, M.U., and Hatano, Y. (2002) Photoabsorption, photoionization, and neutral-dissociation cross sections of simple hydrocarbons in the vacuum ultraviolet range. *J Electron Spectros Relat Phenomena* 123:225–238.

Krasnopolsky, V.A. and Cruikshank, D.P. (1999) Photochemistry of Pluto's atmosphere and ionosphere near perihelion. *J Geophys Res* 104:21979–21996.

Kroll, J.H., Donahue, N.M., Jimenez, J.L., Kessler, S.H., Canagaratna, M.R., Wilson, K.R., Altieri, K.E., Mazzoleni, L.R., Wozniak, A.S., Bluhm, H., Mysak, E.R., Smith, J.D., Kolb, C.E., and Worsnop, D.R. (2011) Carbon oxidation state as a metric for describing the chemistry of atmospheric organic aerosol. *Nat Chem* 3:133–139.

Lavvas, P., Yelle, R.V., and Vuitton, V. (2009) The detached haze layer in Titan's mesosphere. *Icarus* 201:626–633.

Lavvas, P., Galand, M., Yelle, R.V., Heays, A.N., Lewis, B.R., Lewis, G.R., and Coates, A.J. (2011) Energy deposition and primary chemical products in Titan's upper atmosphere. *Icarus* 213:233–251.

Le Picard, S.D., and Canosa, A. (1998) Measurement of the rate constant for the association reaction $CH + N_2$ at 53 K and its relevance to Triton's atmosphere. *Geophys Res Lett* 25: 485–488.

Le Picard, S.D., Canosa, A., Rowe, B.R., Brownsword, R.A., and Smith, I.W.M. (1998) Determination of the limiting low pressure rate constants of the reactions of CH with N_2 and CO: a CRESU measurement at 53 K. *Journal of the Chemical Society, Faraday Transactions* 94:2889–2893.

Lodriguito, M.D., Lendvay, G., and Schatz, G.C. (2009) Trajectory surface-hopping study of methane photodissociation dynamics. *J Chem Phys* 131, doi.org/10.1063/1.3271242.

Matthews, C.N. (1992) Dark matter in the Solar System—hydrogen cyanide polymers. *Orig Life Evol Biosph* 21:421–434.

McDonald, G.D., Thompson, W.R., Heinrich, M., Khare, B.N., and Sagan, C. (1994) Chemical investigation of Titan and Triton tholins. *Icarus* 103:137–145.

McLafferty, F.W. and Turecek, F. (1993) *Interpretation of Mass Spectra*, University Science Books, Sausalito, CA.

Miller, J.A. and Walch, S.P. (1997) Prompt NO: theoretical prediction of the high-temperature rate coefficient for $CH + N_2 \rightarrow HCN + N$. *International Journal of Chemical Kinetics* 29:253–259.

Moskaleva, L.V., Xia, W.S., and Lin, M.C. (2000) The $CH + N_2$ reaction over the ground electronic doublet potential energy

surface: a detailed transition state search. *Chem Phys Lett* 331:269–277.

Mount, G.H., Warden, E.S., and Moos, H.W. (1977) Photoabsorption cross-sections of methane from 1400 to 1850 A. *Astrophys J* 214:L47–L49.

Pavlov, A.A., Brown, L.L., and Kasting, J.F. (2001) UV-shielding of NH_3 and O_2 by organic hazes in the Archean atmosphere. *J Geophys Res* 106:23267–23287.

Phillips, R.J. (1990) Collision-theory treatment of the reactions of CH_3^+ with H_2, D_2, N_2, O_2, NO, CO, CO_2, HCN, and NH_3. *J Phys Chem* 94:5265–5271.

Raulin, F., Mourey, D., and Toupance, G. (1982) Organic synthesis from CH_4-N_2 atmospheres—implications for Titan. *Orig Life Evol Biosph* 12:267–279.

Sagan, C., Thompson, W.R., and Khare, B.N. (1992) Titan: a laboratory for prebiological organic-chemistry. *Acc Chem Res* 25:286–292.

Scalo, J., Kaltenegger, L., Segura, A.G., Fridlund, M., Ribas, I., Kulikov, Y.N., Grenfell, J.L., Rauer, H., Odert, P., Leitzinger, M., Selsis, F., Khodachenko, M.L., Eiroa, C., Kasting, J., and Lammer, H. (2007) M stars as targets for terrestrial exoplanet searches and biosignature detection. *Astrobiology* 7:85–166.

Scattergood, T.W., McKay, C.P., Borucki, W.J., Giver, L.P., Vanghyseghem, H., Parris, J.E., and Miller, S.L. (1989) Production of organic compounds in plasmas: a comparison among electric sparks, laser-induced plasmas, and UV light. *Icarus* 81:413–428.

Segura, A., Kasting, J.F., Meadows, V., Cohen, M., Scalo, J., Crisp, D., Butler, R.A.H., and Tinetti, G. (2005) Biosignatures from Earth-like planets around M dwarfs. *Astrobiology* 5:706–725.

Segura, A., Meadows, V.S., Kasting, J.F., Crisp, D., and Cohen, M. (2007) Abiotic formation of O_2 and O_3 in high CO_2 terrestrial atmospheres. *Astron Astrophys* 472:665–679.

Segura, A., Walkowicz, L.M., Meadows, V., Kasting, J., and Hawley, S. (2010) The effect of a strong stellar flare on the atmospheric chemistry of an Earth-like planet orbiting an M dwarf. *Astrobiology* 10:751–771.

Smith, D. and Adams, N.G. (1978) Molecular synthesis in interstellar clouds: radiative association reactions of CH_3^+ ions. *Astrophys J* 220:L87–L92.

Snijder, E.D., te Riele, M.J.M., Versteeg, G.F., and van Swaaij, W.P.M. (1995) Diffusion coefficients of CO, CO_2, N_2O, and N_2 in ethanol and toluene. *J Chem Eng Data* 40:37–39.

Tao, F.M., Klemperer, W., McCarthy, M.C., Gottlieb, C.A., and Thaddeus, P. (1994) An *ab initio* study of the HNCN radical. *J Chem Phys* 100:3691–3694.

Tian, F., Toon, O.B., Pavlov, A.A., and De Sterck, H. (2005) A hydrogen-rich early Earth atmosphere. *Science* 308:1014–1017.

Tian, F., Kasting, J.F., and Zahnle, K. (2011) Revisiting HCN formation in Earth's early atmosphere. *Earth Planet Sci Lett* 308:417–423.

Toupance, G., Bossard, A., and Raulin, F. (1977) Far UV irradiation of model prebiotic atmospheres. *Orig Life Evol Biosph* 8:259–266.

Trainer, M.G., Pavlov, A.A., Curtis, D.B., McKay, C.P., Worsnop, D.R., Delia, A.E., Toohey, D.W., Toon, O.B., and Tolbert, M.A. (2004a) Haze aerosols in the atmosphere of early Earth: manna from heaven. *Astrobiology* 4:409–419.

Trainer, M.G., Pavlov, A.A., Jimenez, J.L., McKay, C.P., Worsnop, D.R., Toon, O.B., and Tolbert, M.A. (2004b) Chemical composition of Titan's haze: Are PAHs present? *Geophys Res Lett* 31, doi:10.1029/2004GL019859.

Trainer, M.G., Pavlov, A.A., DeWitt, H.L., Jimenez, J.L., McKay, C.P., Toon, O.B., and Tolbert, M.A. (2006) Organic haze on Titan and the early Earth. *Proc Natl Acad Sci USA* 103:18035–18042.

Tran, B.N., Force, M., Briggs, R.G., Ferris, J.P., Persans, P., and Chera, J.J. (2008) Titan's atmospheric chemistry: photolysis of gas mixtures containing hydrogen cyanide and carbon monoxide at 185 and 254 nm. *Icarus* 193:224–232.

Vuitton, V., Yelle, R.V., and McEwan, M.J. (2007) Ion chemistry and N-containing molecules in Titan's upper atmosphere. *Icarus* 191:722–742.

Vuitton, V., Yelle, R.V., and Cui, J. (2008) Formation and distribution of benzene on Titan. *J Geophys Res* 113, doi:10.1029/2007je002997.

Walkowicz, L.M., Johns-Krull, C.M., and Hawley, S.L. (2008) Characterizing the near-UV environment of M dwarfs. *Astrophys J* 677:593–606.

Wilson, E.H. and Atreya, S.K. (2000) Sensitivity studies of methane photolysis and its impact on hydrocarbon chemistry in the atmosphere of Titan. *J Geophys Res* 105:20263–20273.

Wilson, E.H. and Atreya, S.K. (2004) Current state of modeling the photochemistry of Titan's mutually dependent atmosphere and ionosphere *J Geophys Res* 109, doi:10.1029/2003JE002181.

Wolf, E.T. and Toon, O.B. (2010) Fractal organic hazes provided an ultraviolet shield for early Earth. *Science* 328:1266–1268.

Yung, Y.L., Allen, M., and Pinto, J.P. (1984) Photochemistry of the atmosphere of Titan: comparison between model and observations. *Astrophys J Suppl Ser* 55:465–506.

Address correspondence to:
Melissa G. Trainer
NASA Goddard Space Flight Center
Planetary Environments Laboratory
Code 699
Greenbelt, MD 20771

E-mail: melissa.trainer@nasa.gov

Submitted 14 December 2011
Accepted 20 February 2012